

Basis for the Bauschinger Effect in Copper Single Crystals: Changes in the Long-Range Internal Stress with Reverse Deformation.

L.E. Levine, M. R. Stoudt, A. Creuziger
Materials Measurement Laboratory
National Institute of Standards and Technology
100 Bureau Dr, STOP 8553
Gaithersburg, MD 20899-8553 USA
lyle.levine@nist.gov
mark.stoudt@nist.gov
adam.creuziger@nist.gov

T.Q. Phan
Engineering Laboratory
National Institute of Standards and Technology
100 Bureau Dr., STOP 8220
Gaithersburg, MD 20899-8220 USA
thien.phan@nist.gov

Ruqing Xu
Advanced Photon Source
Argonne National Laboratory
Argonne, IL 60439-4800, USA
ruqingxu@aps.anl.gov

M.E. Kassner*
Dept. of Chemical Engineering and Materials Science
RTH 502
Univ. Southern California
Los Angeles, CA 90089
USA
kassner@usc.edu

*corresponding author

Keywords: Bauschinger effect, work hardening, fatigue, internal stress

Abstract

The long range internal stresses (LRIS) associated with the Bauschinger effect were investigated using synchrotron x-ray microbeam diffraction and reversed deformation

experiments. [100]-oriented Cu single crystals were deformed in compression to approximately -0.3 true strain, followed by tension to a strain of approximately +0.02. Two conclusions are arrived at from this work: first, the LRIS are confirmed in this work to be small relative to the applied stress both before and after reversal. Second, the LRIS persist after 2 % reversed strain despite a significant drop in the overall dislocation density by dynamic recovery. This appears to satisfy the necessary condition for LRIS to significantly contribute to a Bauschinger effect in materials. The pronounced Bauschinger effect in Cu is probably best rationalized by a combination of both the LRIS and the Orowan-Sleeswyk model that relies on a non-uniform distribution of dislocation obstacles without a substantial LRIS.

Keywords: X-ray diffraction, dislocation structure, Bauschinger effect, plasticity, internal stress

Introduction

The Bauschinger effect occurs when, after strain hardening, a reversal of the strain direction leads to “early” yielding; isotropic hardening is not observed. The flow stress (yield stress) in the reverse direction appears “premature”. An understanding of the Bauschinger effect is important for cyclic deformation as it may explain stress saturation at the relatively low stresses at which persistent slip bands (PSB) often form, leading to extrusions/intrusions and fatigue cracking. The Bauschinger effect is also important for understanding springback in metal forming.

Currently, there are two main explanations for the Bauschinger effect: one involves long range internal stresses (LRIS) and another relies on the heterogeneous distribution of dislocation-obstacles independent of long range internal stresses (LRIS). Mughrabi [1] and Pedersen [2] suggested that high dislocation-density regions such as cell walls, persistent-slip-band dislocation-

walls and dipole-bundles are associated with relatively high yield stresses, while the lower dislocation-density regions (e.g. cell interiors) have lower yield stresses simply through the Taylor equation for dislocation hardening [3]. During plastic deformation, these “hard” and “soft” regions are compatibly sheared. Since the flow stresses are different, dislocations must exist between these two regions giving rise to the heterogeneous stress-state.

Such a composite model was suggested to rationalize the Bauschinger effect. For example, as soft and hard regions are unloaded from a tensile stress state, the hard region eventually places the soft region in compression while the hard region is still under positive stress. Thus, the Bauschinger effect occurs on stress reversal because the soft regions plastically deform earlier than would be expected for the isotropic case. A very simplified composite model for LRIS [1] and the associated Bauschinger effect is illustrated in Fig. 1(a). LRIS appear as local deviations from the applied stress in a loaded material. In Fig. 1(a):

$$\tau_w^y = \tau_a + \Delta\tau_w \quad (1)$$

$$\tau_I^y = \tau_a + \Delta\tau_I \quad (2)$$

where τ_w^y is the yield stress of the dislocation walls, τ_I^y is the yield stress of the dislocation cell interiors, τ_a is the applied stress, and $\Delta\tau_w$ and $\Delta\tau_I$ are the LRIS in the composite structure. It should be emphasized that this simple schematic is idealized and is just an example of how LRIS can lead to a Bauschinger effect. In reality, Fig. 1 may not be perfectly representative of complicated dislocation microstructures and may preclude conclusions regarding the magnitude of LRIS that can lead to a Bauschinger effect.

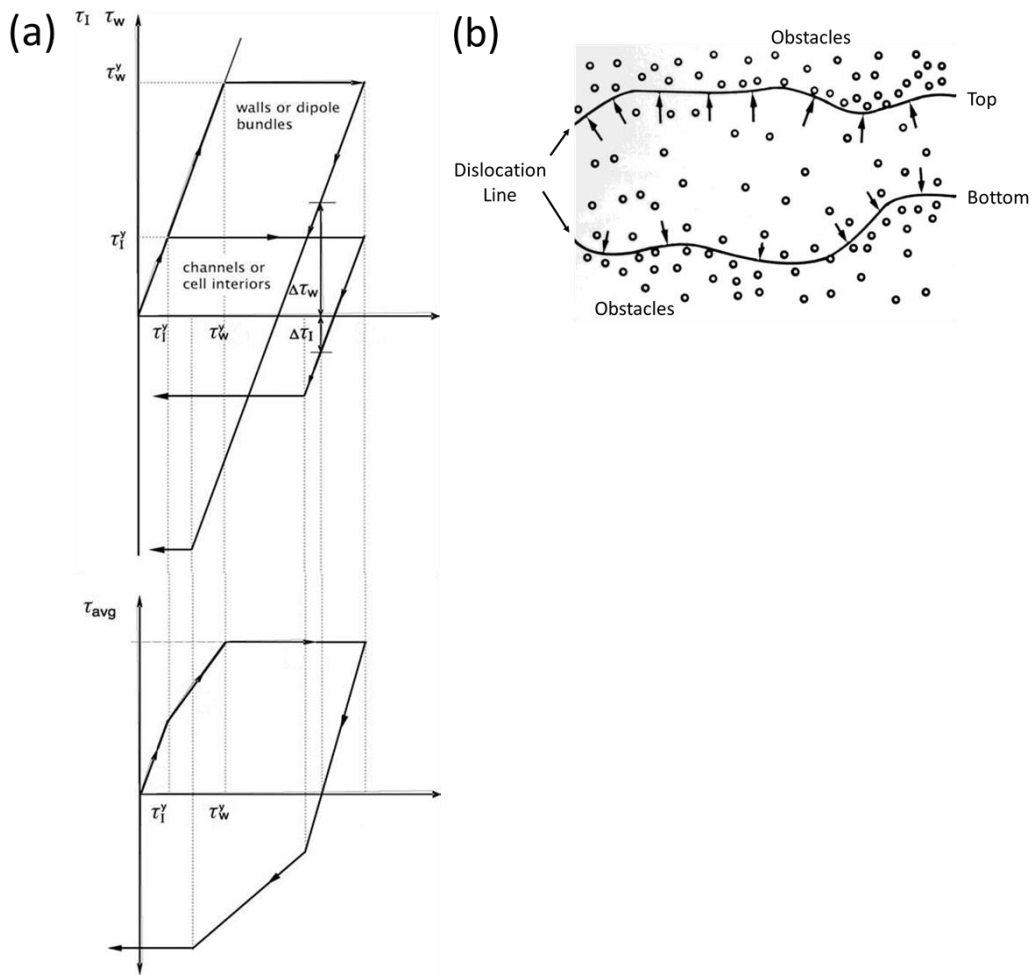


Fig. 1. (a) The stress versus strain behavior according to the composite model of Mughrabi. The top section shows the separate behavior of the cell walls, τ_w , and cell interiors, τ_i , and the bottom section shows the average behavior, τ_{avr} . (b) The Orowan-Sleswyk model where the glide dislocation advances in the forward sense (up in diagram) and eventually encounters a relatively high linear density of obstacles (Top). On reversal, the dislocation glides a relatively large distance (strain) before it encounters the same density of dislocation-obstacles (Bottom) in the forward sense (cell walls). From [5] and [14].

The Orowan-Sleswyk model, on the other hand, considers the Bauschinger effect to be essentially independent of any LRIS (whether they exist or not). Rather, it is a consequence of a non-uniform distribution of dislocation-obstacles such as in Fig. 1(b) [4,5]. Gliding dislocations encounter an increasing (linear) density of dislocations and the flow stress increases. On reversal,

however, the obstacle spacing for the same gliding dislocations is much less and the flow stress, at least initially, is less than for “forward” slip. Eventually, the reversed gliding dislocation will encounter a similar spacing of dislocations as with the forward sense just prior to unloading. Sleeswyk et al. [4] suggested that this would occur after a reverse strain, β , of about 0.01 to 0.03 plastic strain, depending on the material. Interestingly, at saturation of the flow stress, this value of β doubles, possibly coincident with the formation of cell walls (and possible LRIS) which could be associated with dislocations passing from one (e.g.) cell wall to the opposite side of the cell. This is illustrated in Fig. 2. Here, the Bauschinger effect is suggested to be configurational and principally a consequence of the dislocations arranged in a non-uniform, array.

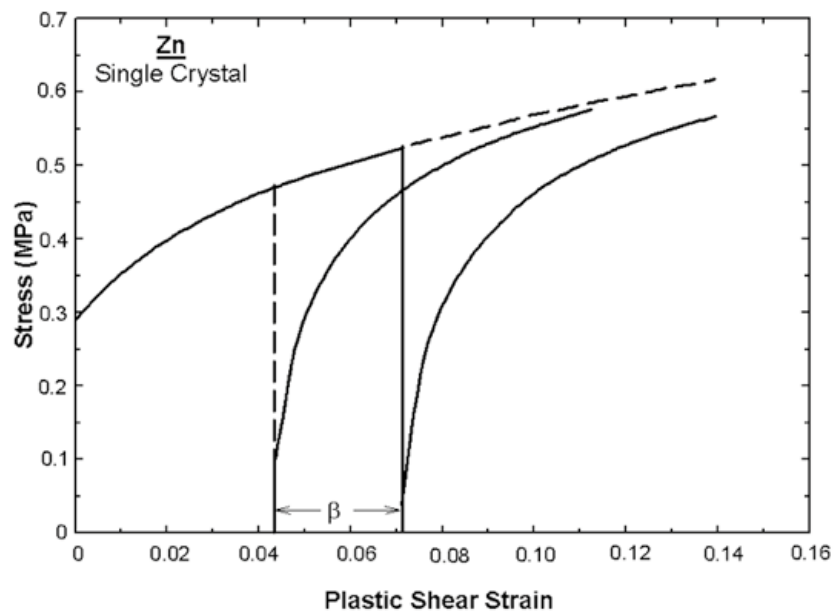


Fig. 2 Subtracting the reverse strain, β , from the cumulative strain after the first reversal causes the reverse curve to approach the extrapolated forward curve in zinc single crystals [4].

There is a similarity between the microstructures discussed by Orowan-Sleeswyk and Mughrabi. The difference between the two is in approach. The microstructures discussed by Mughrabi and Orowan and Sleeswyk have strong similarities, but the Mughrabi composite model relies on the LRIS to rationalize the Bauschinger effect whereas the Orowan-Sleeswyk model does not.

Earlier work by one of the authors measured the Bauschinger effect in 304 stainless steel at elevated temperature as a function of strain [6] and found that the Bauschinger effect becomes more pronounced as the strain increases, coincident with the development of a cellular substructure evident using transmission electron microscopy (TEM). It is important to note that, in this work, a pronounced Bauschinger effect is evident even when TEM reveals an absence of a cellular substructure at a strain of 0.05. It should also be mentioned that in both high-purity Cu single crystals at ambient temperature [7,8] and in high-purity polycrystalline Al at 77K [9], a pronounced Bauschinger effect is observed after initial strains of less than one percent and before dislocation cell walls are expected to be established. Laird [8] illustrates that undeformed Cu single crystals oriented for single slip show a dramatic Bauschinger effect after just 0.005 plastic strain.

These observations demonstrate that the Bauschinger effect can occur in the absence of a cellular substructure but may become more pronounced with the development of dislocation cells/subgrains with coincident LRIS. Thus, it appears feasible that both the Orowan-Sleeswyk model as well as the composite model are relevant to the Bauschinger effect.

A critical requirement for the relevance of the composite model to the Bauschinger effect is that the LRIS must be present during reverse deformation over a strain range comparable to the reversible strain, β . An objective of this research is to assess the LRIS over this reverse strain

range (e.g. 2 %). A persistence of the LRIS over β is a *necessary* condition for the LRIS to rationalize the Bauschinger effect in the [100] oriented Cu single crystals.

Earlier work by the authors [10,11] examined the long range internal stresses in [100] copper single crystals deformed to compressive and tensile true strains of about ± 0.3 . Changes in the lattice parameter along the [100] direction (compression/tension axes) were measured using synchrotron x-ray microdiffraction (the experimental procedure is discussed in [10,11] by the authors). The experimental procedure allowed lattice parameter measurements within a three-dimensional (3D) sample volume that was roughly cubical with an edge size of approximately 0.5 μm (i.e often a “cube” that can fit within a single dislocation cell).

Lattice parameter measurements were performed on individual cell interiors and individual cell walls [11]. It was concluded that the LRIS were about ± 0.10 the applied stress (τ_a) in both the cell interiors and the cell walls; the stresses in the walls and cells have opposite sign and the applied stress was about ± 210 MPa. The dislocations are arranged in low-misorientation ($\theta < 0.1^\circ$) cells with the volume fraction of cell walls approximately equal to that of the low dislocation-density cell interiors. As Eqs. 1 and 2 suggest, and as mentioned earlier, the LRIS are defined here as the difference between the applied stress and the local stress in the microstructure. Thus, the LRIS are simply the local stresses in the unloaded state of the deformed Cu crystal.

This study examines the values of the long range internal stresses both after about 0.3 strain in compression (to compare with our earlier work that was previously discussed) and, for the first time, after reversal to 0.02 strain in tension (within the 0.02 to 0.03 strain range over which the Bauschinger effect is typically observed) in [100] oriented Cu single crystals. As described above, this will further test the viability of the composite model as a path to rationalize the Bauschinger

effect. This requirement is absent for the Orowan-Sleeswyk model; only a heterogeneous distribution of obstacles is critical.

Experimental Procedure

Two nominally identical, [100]-oriented, dogbone-shaped, 99.999% pure, Cu single crystals were deformed in a mechanical testing machine fitted with a digital image correlation (DIC) system. Both samples were deformed in compression to approximately -0.3 true strain. The second specimen was subsequently deformed in tension. Deforming first in compression allowed us to compare the results to previous compression-only results [11], although this choice is contrary to how the composite model is typically introduced and is shown in Fig. 2. The sample geometry and substantial work hardening resulted in some variation in the strain fields, mainly via localized macroscopic shear that developed near the ends of the reduced parallel length. A cross section of each sample was selected for further analysis and informed the DIC data analysis. Both samples were cut in half using electrical discharge machining (EDM) perpendicular to the deformation axis in the center of the gage section. The recast layer was removed using electropolishing and microbeam x-ray diffraction verified that all surface damage was removed.

Fig. 3 shows the true stress – true strain behavior from the compression + tension sample. True strain values were extracted from an approximately 0.7 mm x 0.7 mm square region on the sample surface with the center aligned to the location of microbeam analysis. True stress was calculated using the applied load, initial cross-sectional area, and the average of true strain values parallel to the applied load on a line perpendicular to the loading direction and passing through the area used for strain measurements. The reported strain includes elastic and plastic components, and is likely a lower bound on the strain due to the size of the correlation window and strain

filtering parameters. As shown for the compression + tension data in Fig. 3, the measured true strain in compression was approximately -0.328 with a flow stress of -245 MPa, and a tensile strain of approximately +0.02 following unloading. It should be mentioned that the specimen ends are constrained in this sample geometry, with significant barreling and triaxiality likely causing additional axial stress and contributing to the larger -245 MPa stress than the -210 MPa stress measured in our earlier compression work, where the constraint was minimal. Early deviations from linear elastic behavior in Fig. 3, on reversal, may not be fully reliable and the elastic modulus in Fig. 3 is low. This, notwithstanding, the pronounced Bauschinger effect is clearly evident. Careful repeated reversed mechanical testing by Sauzay [16] and Gong et al. [17] for [100]-oriented Cu single crystals and by the authors on Cu single crystals oriented for single slip [7] show that copper single crystals evince a very pronounced Bauschinger effect at low strain levels. Fig. 3 simply verifies our reverse deformation experiments and illustrates a pronounced Bauschinger effect.

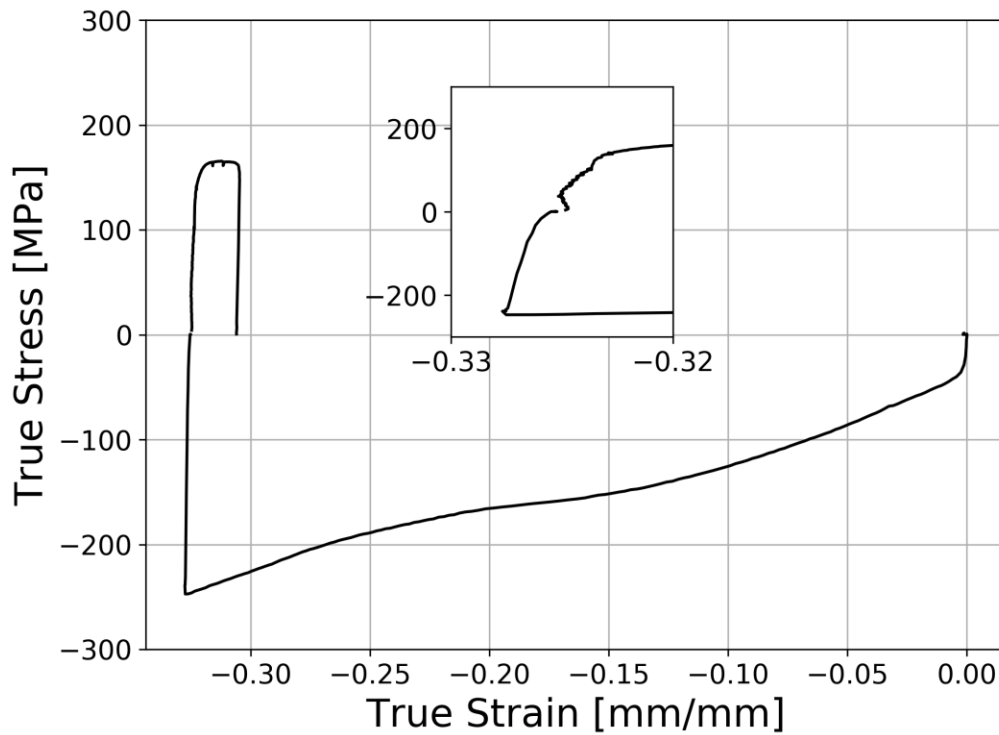


Fig 3. True strain versus true stress data for the compression + tension sample. Inset shows details of the stress versus strain behavior on reversal.

Microbeam diffraction measurements were performed at the 34ID-E beamline at the Advanced Photon Source (APS), Argonne National Laboratory. The experimental methods used were virtually identical to those described elsewhere [11]. Briefly, the incident X-ray beam was converged to $\approx 0.5 \mu\text{m}$ cross-sectional diameter using crossed Kirkpatrick Baez focusing optics. Using a translating monochromator, the incident beam can be polychromatic or monochromatic, with an adjustable energy from about 12 keV to 24 keV. The incident beam intersected the cut surface of the samples at 45° and the diffracted intensity from the axial (600) reflection was detected using a 2D X-ray detector. A high spatial resolution of $\approx 0.5 \mu\text{m}$ within the sample along the beam path was obtained using a translating, depth profiling, platinum wire

that is scanned across the sample surface, blocking diffracted intensity from the sample. The depths from which the X-rays originate are then determined by triangulation.

For these measurements, the profiling wire and X-ray energy scans were conducted to obtain diffraction line profiles from multiple individual dislocation cell interiors; the X-ray energy was scanned from 13.5 keV to 14.5 keV in 3 eV steps, allowing absolute (006) lattice parameters to be measured. Cell interior line profiles were then summed to obtain a cell-interior subpeak. Seventy independent cell interior line profiles were measured from the compression-only specimen and 68 were measured from the compression-tension specimen. Previous studies have demonstrated that this is an adequate sampling of the cell interior strains [11,18]. Monochromatic scans from the same sample volumes without the depth-resolving wire were conducted to measure the shapes of the line profiles for all the material along the beam path (including both cell interiors and cell walls). As mentioned earlier, detailed transmission electron microscopy and x-ray diffraction measurements were conducted on these and similar samples demonstrating that the ratio of cell-wall to cell-interior volume is close to 1:1 [11]. Scaling the cell interior subpeak using this ratio and subtracting from the measured complete-material profile allows the cell-wall subpeak to be extracted. This procedure was tested using data obtained from [11], providing essentially indistinguishable results.

Results and Discussion

The results are illustrated in Figs. 3 and 4. Fig. 3 shows the true stress, true strain data upon reversed deformation in the [100] oriented Cu single crystal and a pronounced Bauschinger effect is evident; even after 2 % reversed strain, the flow stress did not return to the same (opposite sign) stress as at unloading from compression. After 2 % strain on reversal, the flow stress is only

about 175 MPa and has not returned to that which was observed prior to unloading of about 250 MPa. It also can be noted that some non-elastic reversed strain ($< 10^{-3}$) is evident at unloading to zero stress, but as mentioned earlier, the authors do not believe that conclusions based on the early strains on reversal (i.e. much less than 2 %) are possible.

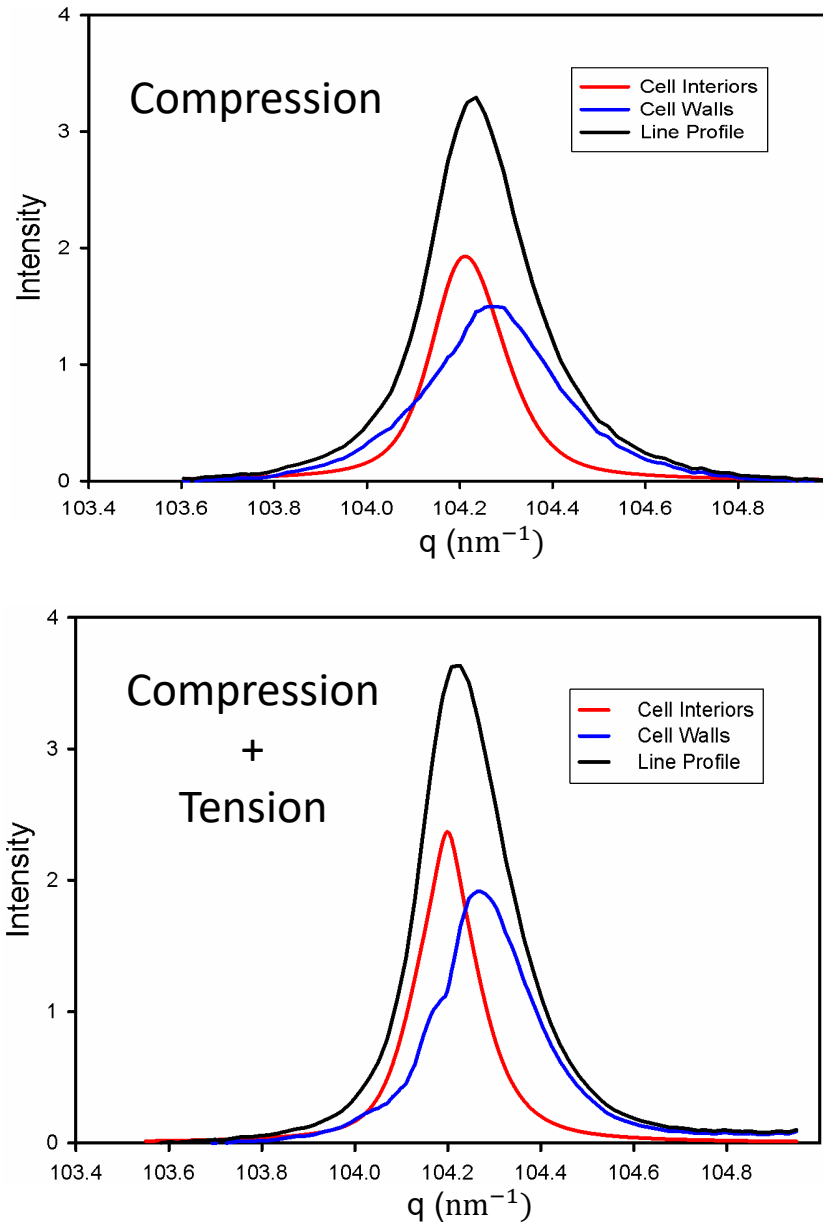


Fig. 4. (a) The x-ray peaks of the cell interiors and cell walls in [100] oriented Cu single crystal unloaded after a strain of -0.328. (b) The peak profiles after a + 0.02 strain in tension, which show

narrowing but unchanged position (same LRIS) from (a). $q = |\mathbf{q}| = (4\pi/\lambda)\sin\theta$, where \mathbf{q} is the scattering vector, λ is the X-ray wavelength, and θ is the Bragg angle.

The LRIS values are listed in Table 1 and are in excellent agreement with our earlier compression studies. Fig. 4(a) shows the X-ray line profile and subpeaks in the compression sample. Fig. 4(b) illustrates the x-ray line profile and subpeaks from the compression + tension specimen. We notice that, on reversal, the three peaks sharpen; they are significantly narrower than the diffraction peaks from the compression-only sample. The sharpening is likely due to a decrease in dislocation density after tensile deformation, presumably by dynamic recovery. However, the LRIS is *unchanged* since the position of the peaks is unchanged (see Table 1).

Table 1: Measured stress differences between the mean cell interior stresses and mean cell wall stresses in Cu single crystals deformed along a [001] crystallographic axis.

	LRIS (full range)
Compression (from ref. [2])	(40 ± 3) MPa
Compression (this work)	(42 ± 3) MPa
Compression + Tension	(42 ± 3) MPa

The observation that the subpeak peak positions remain unchanged while reducing in width implies that, during reversal, substantial dislocation recovery occurs but the dislocations within the cell walls that are responsible for the dipolar LRIS are stable after a reversed deformation to +0.02 strain. This persistence is a necessary condition in order for the composite model to contribute to the Bauschinger effect.

Thus, the necessary condition that the LRIS persist over a range of strain from 0.1-0.3 appears to be satisfied for the composite model. On one hand, one might argue that for equal

volume fractions of cell wall and cell interiors, Fig. 1 suggests that LRIS in the wall that is *two or three times* larger than the applied stress could roughly model the Cu Bauschinger experiments in this and the referenced works. However, as discussed earlier, the model in Fig. 1 is very simplified and probably cannot be used to predict the Bauschinger effect in actual dislocation microstructure based on LRIS. Thus, in the case of Cu, the Orowan-Sleeswyk model that does not explicitly rely on LRIS appears more attractive in rationalizing the Bauschinger effect than the composite model at *early* strain where a cellular substructure is not developed. At larger strains where both β and σ_b increase markedly with the development of a cellular/dipole-vein substructure, LRIS as evolved from the cells/subgrains the composite model may make a substantial contribution of the Bauschinger effect. A more precise appropriation of the contributions of the two models is not possible at this point. Some small portion of the Bauschinger effect in Cu can probably be explained by anelastic unbowing of dislocation segments. Anelastic unbowing of dislocations is expected to be complete on unloading to zero stress corresponding to a strain much less than 0.02. The stress associated with the onset of reversed plasticity may not, by itself, lead to a meaningful description of the Bauschinger effect as multiple processes are involved.

Conclusions

Two [001]-oriented Cu single crystals were deformed in compression to a strain of about -0.3 and one was subsequently reverse deformed in tension to a strain of about +0.02. Synchrotron x-ray microbeam diffraction was used to measure the axial elastic strains within dislocation cell interiors in the compression and in the compression-tension samples, allowing the cell interior and cell wall subprofiles to be obtained. The observed LRIS persists over a reversed plastic strain of +0.02, despite an overall decrease in the dislocation density, as evidenced by the decreased profile

widths. This satisfies a necessary condition for the composite model to explain/contribute to the Bauschinger effect. In the case of where cellular substructures do not form at early strains (e.g. less than 1% strain in at least the systems referenced, and the observation of a very pronounced Bauschinger effect suggests that at least some of the Bauschinger effect can be rationalized by the Orowan-Sleeswyk model. With increasing strain prior to reversal, the Bauschinger effect as measured by σ_b and β (approximate “depth and width” on a stress versus strain plot) suggest that the composite model leading to LRIS is also contributing to the Bauschinger effect.

Acknowledgements

The support by the National Science Foundation under grant DMR-1401194 is greatly appreciated. This research used resources of the Advanced Photon Source (beamline 34-ID-E), a U.S. Department of Energy Office of Science User Facility operated for the DOE Office of Science by Argonne National Laboratory under Contract No. DE-AC02-06CH11357. There are no competing interests by any of the authors.

References

- [1] Mughrabi H, (1983) Dislocation Wall and Cell Structures and Long-range Internal Stress In Deformed Metal Crystals, *Acta Metall*, 31:1367-1379.
- [2] Pedersen OB, Brown LM, Stobbs WM (1981) The Bauschinger Effect in Copper, *Acta Metall*, 29:1843-1850.
- [3] Kassner ME (1990) A Case for Taylor Hardening During Primary and Steady-State Creep in Aluminum and Type 304 Stainless Steel, *Jour. of Mater. Science*, 25:1997-2003.
- [4] Sleeswyk AW, James MR, Plantinga DH, Maathius WST (1978), Reversible strain in cyclic plastic deformation, *Acta Metall*. 26:1265-1271.

- [5] Orowan E (1959), Internal Stresses and Fatigue in Metals, in: General Motors Symposium, G.M. Rassweiler, W.L. Grube eds, Elsevier, Amsterdam, pp. 59.
- [6] Kassner ME, Ziaai-Moayyed AA, Miller AK (1985) "Some Trends Observed in the Elevated Temperature Kinematic and Isotropic Hardening of Type 304 Stainless Steel," *Metall. Trans.* 16A:1069-1076.
- [7] Kassner ME, Perez-Prado M-T, Vecchio KS, Wall MA (2000), Determination of Internal Stresses in Cyclically Deformed Cu Single Crystals Using CBED and Dislocation Dipole Separation Measurements, *Acta Mater*, 48:4247-4254.
- [8] C. Laird (1983) The Application of Dislocation Concept in Fatigue, *Dislocations in Solids*, vol. 6. Nabarro, F.R.N. (Ed.), North Holland, Amsterdam pp. 55-120.
- [9] M.A. Delos Reyes, MS Thesis, Dept. of Mechanical Engineering, Oregon State Univ, Corvallis, OR USA, 1995.
- [10] Levine LE, Larson BC, Yang W, Kassner ME, Tischler JZ, Delos-Reyes MA, Fields RJ, (2006) X-ray Microbeam Measurements of Individual Cell Elastic Strains in Deformed Single Crystal Copper, *Nature Materials* 5:619-622.
- [11] Levine LE, Geantil P, Larson BC, Tischler JZ, Kassner ME, Liu, W, Stoudt MR, Tavazza F (2011) Disordered Long-range Internal Stresses in Deformed Copper and the Mechanisms Underlying Plastic Deformation, *Acta Mater*, 59:5083-5091.
- [12] Seeger A (1957), Glide and Work Hardening in Face-centered Cubic and Hexagonal Close-Packed Metals. In: Dislocations and Mechanical Properties of Crystals, J. C. Fisher, W.G. Johnston, R. Thomson and T. Vreeland eds, Wiley, New York, 243.
- [13] Borbély, A, Blum, W, Ungar, T. (2000), On the Relaxation of the Long-range Internal Stresses of Deformed Copper upon Unloading, *Mater. Sci. Eng*, 276: 186–194.
- [14] Kassner ME, Geantil P, Levine LE and Larson BC (2009), Long-range Internal Stresses in Monotonically and Cyclically Deformed Metallic Single Crystals, *Int. J. Mater. Res.* 100:333-339.
- [15] Mughrabi H (1988), Dislocation Clustering and Long-range Internal Stresses in Monotonically and Cyclically Deformed Metal Crystals, *Rev. de Phys Appliq*, 23:367-379.
- [16] Sauzay M, unpublished research, 2017, CEA/DEN/DANS/DMN/SRMA, Bat. 455, 91191 Gif-sur-Yvette Cedex, France

[17] Gong B, Wang Z, Wang Z (1997), Cyclic Deformation Behavior and Dislocation Structures of [001] Copper Single Crystals-I Cyclic Stress-strain Response and Surface Feature, *Acta Mater*, 45:1365-1377.

[18] Levine LE, Geantil P, Larson BC, Tischler JZ, Kassner ME and W. Liu W (2012) Validating Classical Line Profile Analyses Using Microbeam Diffraction from Individual Dislocation Cell Walls and Cell Interiors, *J. Appl. Cryst.* 45:157-165.

[19] Mughrabi, H, Ungar, T, (2002) "Long Range Internal Stresses in Deformed Single-phase Materials: the Composite Model and its Consequences", *Dislocations in Solids*. Vol. 11, Nabarro, F.R.N. and Hirth J. (Eds.), Elsevier, Amsterdam, p. 343-411.

[20] Kassner M.E (2013) "Long Range Internal Stresses in Single-phase Crystalline Materials" Geantil P, Levine LE, *Inter. Jour. Plast*, 45:44-60.

The only experiment that has assessed relaxation of the LRIS are creep tests using x-ray peak asymmetry changes of alloyed Cu. This experiment suggested that about one-third of the LRIS may relax on cooling to ambient temperature [13].